GeoAmericas2020
4th PAN AMERICAN CONFERENCE ON GEOSYNTHETICS
26-29 APRIL 2020 • RIO DE JANEIRO • BRAZIL

Generalized pullout predictive equations of bearing reinforcement for cohesive-frictional soils at various water contents and fines contents

Suksun Horpibulsuk, Artit Udomchai, School of Civil Engineering, Suranaree University of Technology, Nakhon Ratchasima, Thailand.
Gampanart Sukmak, Patimapon Sukmak, School of Engineering and Technology, Walailuk University, Nakhonsithammarat, Thailand.
Arul Arulrajah, Swinburne University of Technology, Hawthorn, Victoria 3122, Australia.

ABSTRACT
Bearing reinforcement, which is composed of a longitudinal member (steel deformed bar) and transverse (bearing) members (a set of equal angle steel), has been established as an effective earth reinforcement material. The usage of locally available soils as backfill material is particularly cost effective for construction sites where there is a lack of available quality friction (coarse-grained) materials. The pullout resistance of the bearing reinforcement comprises both friction and bearing components. In this research study, the test results of residual red clay and previously published test results were analyzed to develop generalized equations for predicting pullout resistance of bearing reinforcement when embedded in compacted cohesive-friction soils, with various water contents and fines contents. The pullout friction resistance can be calculated by utilizing the soil-reinforcement interaction factor, α, which reduced linearly with fines content (F). The bearing pullout resistance is controlled in the failure plane (β) during the pullout of a single transverse member and. The water content to optimum water content ratio, w/w_{OWC} and F are found to be dominant factors controlling both w/w_{OWC} and IF. The reduced from $\pi/2$ to $\pi/3$ with the increase in w/w_{OWC} and F. Equations for predicting β, in terms of the fines content and water content, were proposed in this paper. In addition, generalized pullout resistance equations in terms of normal stress, shear strength parameters, fines content and water content were also developed. The developed equations are innovative and useful for the internal stability analysis of bearing reinforcement earth walls during and post-construction

Keyword: bearing reinforcement, pullout resistance, cohesive-frictional backfill, fines content, water content.

1. INTRODUCTION

Mechanical stabilized earth (MSE) walls have been proven to be an effective retaining structure in infrastructure applications (Horpibulsuk et al., 2011 and Udomchai et al., 2017). The reinforcement types are classified into inextensible and extensible materials, depending upon the amount of deformation that occurs during loading. The steel reinforcement (i.e. steel strips and steel grid) is inextensible, whilst the polymeric synthetic reinforcement materials (i.e. geotextile and geogrid) are extensible. Both types of reinforcement minimize the horizontal movement of the MSE wall (Jiang et al., 2016; Liu, 2012; Mohamed et al., 2013; Palmeira, 2004; Roodi Gholam and Zornberg Jorge, 2017). The reinforcement can also be placed at base of embankment on soft soil to enhance bearing capacity and reduce the settlement of foundation (Bonaparte and Christopher, 1987; Chai et al., 2002; Jewell, 1988; Zhang et al., 2015)

Horpibulsuk and Niramitkronburee (2010) developed a cost-effective inextensible reinforcement type, termed as “Bearing reinforcement”, which is composed of a longitudinal member and transverse (bearing) members (Figure 1). The longitudinal member is a steel deformed bar and the transverse members are a set of equal steel angles. This reinforcement has the additional advantage of the inclusion of both steel strip and grid reinforcements, which are enhanced by a simple and fast installation technique at the wall facing panel and a high pullout resistance with less steel volume. The earth wall stabilized by bearing reinforcement is designed as a “Bearing Reinforcement Earth (BRE) wall” (Horpibulsuk et al., 2011).

The BRE wall has been developed into a standard mechanically stabilized earth (MSE) wall system for the Department of Highways (DOH) in Thailand and has also been successfully implemented in many construction projects of Department of Highways (DOH), Department of Rural Roads and Electricity Generating Authority of Thailand. The equation to predict pullout resistance of the bearing reinforcement embedded in sand was proposed by Horpibuksuk and Niramitkornburee (2010) based on the pullout apparatus (Figure 1b). The design method was first proposed by Horpibulsuk et al. (2012 and 2013) and Suksiripattanapong et al. (2012) for high quality friction (coarse-grained) backfill according to AASHTO (2002) and DOH’s specification, which specifies a fines content (<0.075 mm), F of less than 15% and a plasticity index of less than 6%.

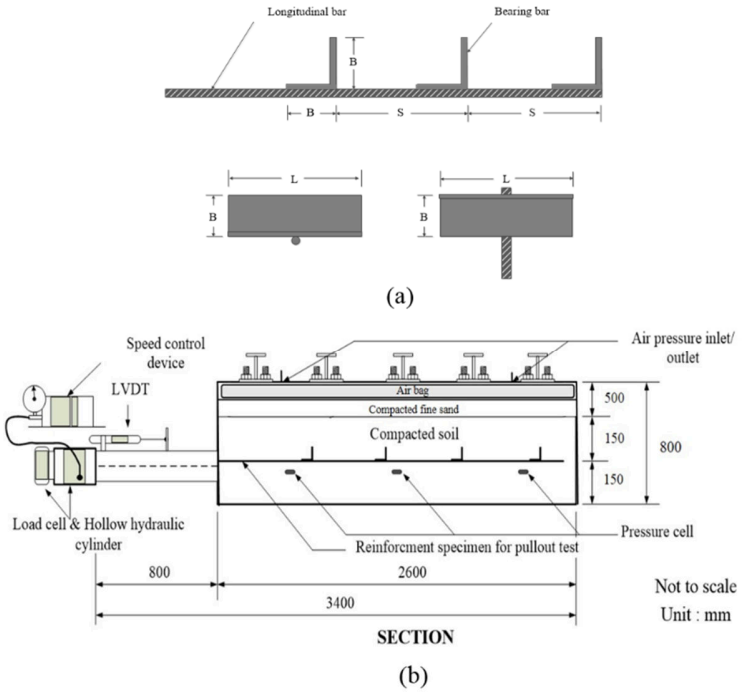

Figure 1 a) Typical schematic view of the bearing reinforcement (form Horpibulsuk and Niramitkornberee, 2010)
b) Pullout test apparatus

The usage of cohesive-frictional soil as a backfill material for BRE walls is challenging, as the generalized pullout resistance equations for cohesive-frictional soil at various water contents and fines contents, are not currently available. Sukmak et al. (2015) investigated the effect of fines contents on pullout resistance of bearing reinforcement embedded in cohesive-frictional soil at various fines contents (F) of 20, 40, 80, and 98% by dry weight. Recently, Horpibulsuk et al. (2016) investigated the pullout resistance of two clayey soils with 98% fines content. However, these two research studies are only applicable for the compacted soils at the optimum water content (w_{owc}) and maximum dry unit weight. Sukmak et al. (2016) investigated the effect of water contents on pullout resistance of bearing reinforcement embedded in clayey sand soil (F = 20%) compacted at various water contents (-2.5%<w_{owc}<2.5%), which are generally specified for the field compaction.

Reanalysis of the available test results taking into account the combined effect of fines content and water content for developing generalized pullout resistance predictive equations is significant and is the focus of this research. To have a better insight, a pullout test result of red clay from this study is also analyzed. The studied water content of red clay is in the range of -2.5%<w_{owc}<2.5%, specified for field compaction according the Department of Highways and Department of Rural Roads, Thailand. This study is based on the total strength parameters, which is acceptable in practice for compacted unsaturated soils (Bergado et al., 1996; Liu et al., 2009; Sukmak et al., 2016; Sukmak et al., 2015). The outcome of this research will lead to the usage of in-situ cohesive-frictional soil as a backfill material for BRE walls, which can substantially reduce costs associated with long distance haulage of imported virgin materials

2. THEORETICAL BACKGROUND

The pullout mechanism for bearing reinforcements consists of two prime components: friction resistance along the longitudinal member and bearing resistance at the front of transverse members (Horpibulsuk and Niramitkronburee, 2010; Suksiripattanapong et al., 2013 and Sukmak et al., 2015, Potyondy, 1961).

The pullout friction resistance of bearing reinforcement (without any transverse member) is the skin friction between soil and longitudinal bar. The friction pullout resistance of longitudinal member, P_f, is expressed in the form of:

$$P_f = \pi D L_e \alpha (c + \sigma_n \tan\phi) \quad [1]$$

where α is the interaction factor, c and ϕ are the total strength parameters (cohesion and internal friction angle) of compacted soil, σ_n is the applied normal stress and D and Le are the diameter and embedded length of the longitudinal member, respectively.

The bearing pullout force, P_{bn} of the transverse members, which are placed at regular intervals, is governed by the interference of each transverse member during pullout. The bearing pullout force, P_{bn} is expressed as:

$$P_{bn} = nIFP_{b1} \quad [2]$$

where n is the number of transverse members, IF is the transverse members interference factor and P_{b1} is bearing pullout force of a single transverse member.

Typically, the leg length, B, of the transverse members (steel equal angles) is smaller than 40 mm, while the length, L, is larger than 150 mm. The L/B value for the transverse members is therefore more than 3.7. Although during pullout of the bearing reinforcement, the deformation around the transverse member is three-dimensional (3D), previous studies (Horpibulsuk and Niramitkornburee, 2010; Suksiripattanapong et al., 2013; Sukmak et al., 2015 and Horpibulsuk et al., 2016) reported that within this B/L range, the three-dimensional effect has been inexplicitly considered by the proposed plane strain failure model (2D). By extending the modified punching shear mechanism (Bergado et al., 1996; Chai, 1992), the P_{b1} can be determined using the following equations.

$$P_{b1} = \left[cN_c + \sigma_n N_q\right]BL \quad [3]$$

$$N_q = \frac{1}{\cos\phi}\exp\left[2\beta\tan\phi\right]\tan\left(\frac{\pi}{4}+\frac{\phi}{2}\right) \quad [4]$$

$$N_c = \frac{1}{\sin\phi}\exp\left[2\beta\tan\phi\right]\tan\left(\frac{\pi}{4}+\frac{\phi}{2}\right) - \cot\phi \quad [5]$$

where B and L are leg length and length of transverse member, respectively (Figure 1), β is the failure angle (radian).

The extensive test results reported previously (Suksiripattanpong et al., 2013; Sukmak et al., 2015 and 2016) that β was dependent upon F and water content ratio (w/w_{OWC}), where w is water content and w_{OWC} is the optimum water content. When the β values are $\pi/1.65$ and $\pi/3$, the failure modes are general shear (Perterson and Anderson, 1980) and punching shear (Jewell et al., 1984) mechanisms, respectively, which are the upper and lower boundary limits.
The transverse members interference factor (IF) on the bearing reinforcement is controlled by the spacing of the transverse members S and B, regardless of L (Horpibulsuk and Niramitkronburee, 2010; Sukmak et al., 2016; Sukmak et al., 2015; Suksiripattanapong et al., 2013). The failure mechanism for the bearing reinforcement was classified into three failure characteristics: block failure, interference failure, and individual failure, depending upon the S/B value as shown in Figure 2.

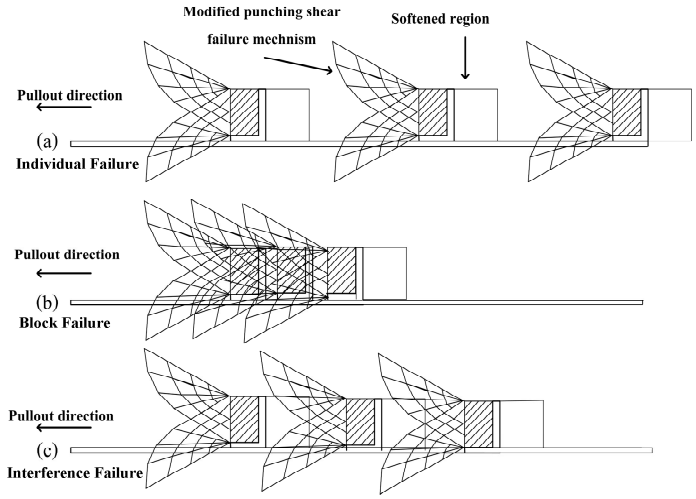

Figure 2 Transverse members interference (from Sukmak et al. 2015)

When the S/B is large, the soil in front of the transverse members fails individually. For the block failure (low S/B), the shear surface caused by each transverse member combines to form a rough shear surface. Only the first transverse member provides bearing resistance. The S_1/B is defined as the spacing ratio, which separates the block failure and the interference failure zones. S_2/B is defined as the spacing ratio, which separates the interference failure and individual failure zones. The transverse members interference results in a softened region to form behind the transverse member where soil failure subsequently occurs. In other words, the larger the softened region, the lower the S_2/B. Based on the extensive past test results, S1/B can be taken as 3.75 for a wide range of fines contents (Sukmak et al., 2015 and 2016 and Horpibulsuk et al., 2016). Sukmak et al (2015) reported that a lower shear strength results in a smaller softened region, and hence a lower S2/B value. The IF is equal to 1/n when $S/B < S1/B$ (block failure) and 1 when $S/B > S_2/B$ (individual failure). When $S_1/B < S/B < S_2/B$, the IF can be determined from logarithm of S/B, irrespective of applied normal stress as follows.

$$IF = a + b\ln\left(\frac{S}{B}\right) \quad [6]$$

$$b = \frac{\left[1-\frac{1}{n}\right]}{\left[\ln\left(\frac{S_2}{B}\right)-1.322\right]} \quad [7]$$

$$a = 1 - b\ln\left(\frac{S_2}{B}\right) \quad [8]$$

The number and spacing of the transverse members are determined based on the internal stability design method of BRE wall suggested by Horpibulsuk and Niramitkornburee, 2010 and Suksiripattanapong et al., 2013 for coarse-grained backfill and Udomchai et al., 2011 for fine-grained backfill. The pullout resistance of each reinforcement must be high enough against pullout failure due to the dead load and live load with factor of safety of 1.5. Typically, the vertical spacing of the MSE wall is 750 mm as suggested by AASHTO (2002) to have good interaction between backfill and reinforcements. For the BRE wall, the reinforcement is connected to the wall facing by a locking bar and the vertical spacing is 750 and 350 mm depending upon the height of BRE wall. The facing panels are made of segmental concrete panel, which measured 1.50x1.50x0.14 m in dimension. The good interaction between backfill and reinforcement in BRE wall has been reported by Horpibulsuk et al. (2011) for coarse-grained backfill and Udomchai et al. (2017) for fine-grained backfill.

3. MATERIALS AND METHODS

3.1 Soil Samples

The tested soil was the residual red clay soil, containing 98% of fines content which was collected from the Mae Moh mine of Electricity Generating Authority of Thailand. The fines content of the tested soil was greater than the limitation of 15%, specified by ASSHTO and Department of Highways, Thailand. The tested soil was classified as a marginal (low quality) soil. According to the Unified Soil Classification System (USCS), the red clay was classified as a high plasticity clay (CH). Its specific gravity was 2.74. The liquid limit and plastic limit were 67% and 24%, respectively. Physical and engineering properties of red clay shows in Table 1.

Table 1 Physical and engineering properties of red clay

Properties of red clay	w_1	w_2	w_3	w_4	w_5
Maximum dry density (kN/m^3)	17.25	17.40	17.60	17.00	15.85
Water content (%)	12	14	16	18	20
Degree of saturation (%)	59	70	83	85	88
Relative degree of compaction (%)	96.36	98.63	100	98.63	96.36
Water content ratio	0.75	0.88	1.00	1.13	1.25
Angle of internal friction, ϕ	13	11	6	5	4
Cohesion, c (kPa)	22	21	19	14	8

The water contents of the tested soil were adjusted by spraying water droplets onto the air-dried soil. The soil samples were then transferred to plastic bags and placed without agitation for about 48 hours to achieve a uniform moisture before compaction testing. The compaction characteristic under standard Proctor energy (ASTM D698-91, 1995) was w_{OWC} = 16% and maximum dry unit weight, $\gamma_{dry,max}$ = 17.61 kN/m^3. The soil samples were prepared for both direct shear and pullout tests at five different molding water contents, w, which were on the dry side of optimum (w_1 = 12% and w_2 = 14%), at w_{OWC} (w_3 = 16%), and on the wet side of optimum (w_4 = 18% and w_5 = 20%). The degrees of saturation,S_r, corresponding to w_1, w_2, w_3, w_4, and w_5 were 59%, 70%, 83%, 85%, and 88%, respectively. On the dry side of optimum, the dry unit weight was not sensitive to the water contents; i.e. it varied within a small range of 17.25 to 17.60 kN/m^3. On the wet side of optimum, the dry unit weight considerably decreased as the water content increased.

The total strength parameters for the tested soil were obtained from a large direct shear device with a dimension of 305 mm x 305 mm x 240 mm depth. The detail of the test has been reported by Sukmak et al. (2015). The soil samples were prepared at the required water contents (w_1, w_2, w_3, w_4, and w_5) and at their corresponding dry unit weight before being transferred to the large direct shear box. The applied normal stresses were 30, 50, 90 kPa, respectively. The test commenced with no time allowed for the sample to consolidate during the applied normal stress and shearing. The shear force was applied at a constant shearing rate of 1 mm/min till the sample was sheared at 40 mm. The soil samples were sheared at a rapid rate to ensure minimal changes in matric suction during the shearing processes (Fleming et al., 2006; Oloo and Fredlund, 1996 and Chinkulkijniwat et al., 2015). For an unsaturated soil, total strength parameters are more appropriate to describe the soil behavior than undrained or drained parameters.

3.2 Bearing Reinforcement

The leg length, B, of the tested transverse members (steel equal angles) were 25, 40, and 50 mm, while the length, L, were 100, 150, and 200 mm, respectively, which are typical to those used for BRE walls. The spacing between the transverse members, S, varied from 150 to 1500 mm, depending upon the number of transverse members. In this study, the number of transverse members, n, was 1 to 4, which is typical in practice. The longitudinal and transverse members are very strongly welded. The welding strength is designed to sustain the load not less than the tensile strength of the longitudinal member, according to the American Institute of Steel Construction (AISC).

3.3 Methodology

The pullout test apparatus used in this investigation was made of rolled steel plates, angles, channels, and H section welded or bolted together to provide an inside dimension of 2.6 m length, 0.6 m width and 0.8 m height. The front wall contained upper and lower portions, with a slot allocated in between for the reinforcement specimen. Friction between the tested soils and the side walls of the apparatus was minimized by using a lubricated rubber member as recommended by Alfaro et al. (1995). To reduce the arching effect near the front wall, a sleeve was installed inside the slot opening, which was 150 mm in horizontal width and 100 mm in height, to isolate the bearing reinforcement near the front wall. A compacted soil thickness of 300 mm was maintained above and below the reinforcement.

A compacted soil thickness of 300 mm was maintained above and below the reinforcement (Figure 1b). The soil compaction for each portion (above and below the reinforcement) was undertaken in two layers (150 mm thickness) by a vibratory compactor until the maximum dry unit weight was attained. Normal stress was applied with a pressurized air bag positioned between the compacted soil and the top cover of the apparatus. Before installing the air bag, a 30 mm thick layer of sand was placed on the top of the compacted soil and covered by a 4 mm thick steel plate. This procedure was undertaken to produce a uniformly distributed normal stress on the top of the backfill soil. The pullout force was applied with a 200 kN capacity electro-hydraulic controlled jack. The pullout displacement at the front to the pullout apparatus was monitored by a linear variation differential transformer (LVDT). The maximum applied pullout displacement (end the test) was 40 mm. The applied normal stress was 30, 50, and 90 kPa.

The pullout tests were conducted at a pullout rate of 1.0 mm per minute as recommended by Sukmak et al. (2015) for unsaturated soils. At least three samples were tested under the same conditions to assure consistency of the test results. In most cases, the results under the same testing conditions were reproducible with a low mean standard deviation, SD (SD/$\bar{x}$ < 10%, where $\bar{x}$ is mean strength value). Besides the red clay, the data from previous research (Sukmak et al., 2015 and 2016 and Horpibulsuk et al., 2016) were taken and reanalyzed to develop the generalized equations for assessing pullout resistance at various water contents and fines contents.

4. TEST RESULTS AND DISCUSSION

4.1 Shear Strength of Compacted Backfills

Figure 3 show the relationships between shear strength and water content ratios (w/w_{OWC}) for red clay (F = 98%) compacted at different water contents, respectively. The shear strength decreased with increasing water content ratio. The linear relationship between shear strength and was observed for red clay. Sukmak et. al, 2015 reported that F = 45% was

the threshold limit that the shear strength sharply decreases with F. The change of shear strength with F was relatively small when F < 45% but was significantly larger when F > 45%. The large decrease in shear strength was clearly noted with higher normal stress. The sudden change in shear strength when F > 45% is because at this condition, the fines particles fill the void spaces between the coarse particles and dominate the coarse-grained behavior (Wang et al. 2009). The large amount of fines particles cause the slippage and sliding of coarse grains. The shear strengths therefore decrease with an increase in fine content due to the decrease of internal friction angle. This understanding of shear strength change is vital for BRE wall design, as the shear strength controls the pullout resistance.

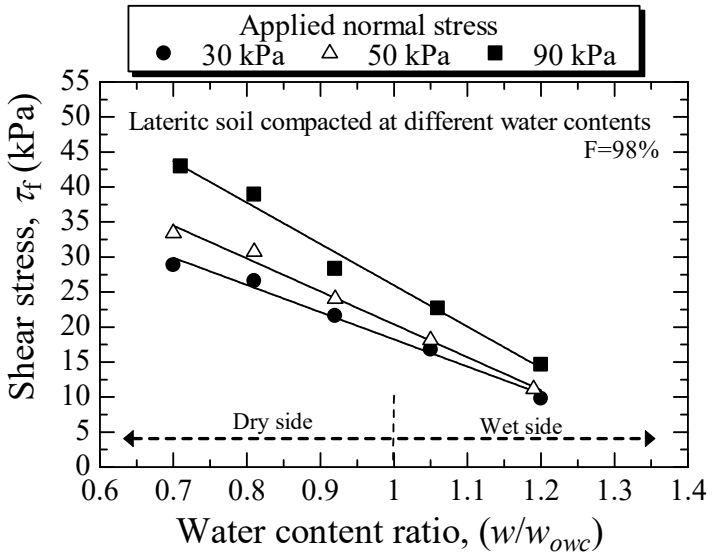

Figure 3 Relationships between shear strength and water content ratios (w/w_{OWC}) of red clay.

4.2 Friction Pullout Resistance

Figure 4 shows the results of the pullout friction tests on a longitudinal member bar with a diameter of 16 mm and a length of 2.6 m embedded in red clay. The friction force increased with the pullout displacement until the peak friction pullout force, $P_{f,peak}$ was reached and subsequently reduced to the end of test of 40 mm. The friction pullout force at the end of test is herein defined as the residual friction pullout force, $P_{f,residual}$. The displacement corresponding to $P_{f,peak}$ was 3-5 mm for all applied normal stresses. The $P_{f,peak}$ and $P_{f,residual}$ increased with an increase of the normal stress and depended upon the water content. The $P_{f,peak}$ and $P_{f,residual}$ values significantly reduced with increasing water content because of the significant reduction in shear strength (see Figure 3).

Figure 5 shows the relationships between the interface shear strength versus shear strength of compacted red clay. From a linear regression analysis, the peak and residual interaction factors (α_p and α_r) of red clay (F = 98%) were 0.66 and 0.47, respectively for all water content tested. These values are close to those (α_p = 0.63 and α_r = 0.46) reported by Sukmak et al. (2015) for high plasticity clay (CH and F = 98%). Based on this present work and previous research (Sukmak et al., 2015 and Horpibulsuk et al., 2016), the α_p and α_r for a particular soil are constant with water contents. Sukmak et al. (2016) have proposed a relationship between α_p and α_r versus F as follows:

$$\alpha_p = -0.002F + 0.859 \quad \text{for } 20 < F < 98\% \quad [9]$$

$$\alpha_r = -0.0014F + 0.592 \quad \text{for } 20 < F < 98\% \quad [10]$$

Both equations are recommended as a quick tool for predicting α_p and α_r at various fines contents and water contents.

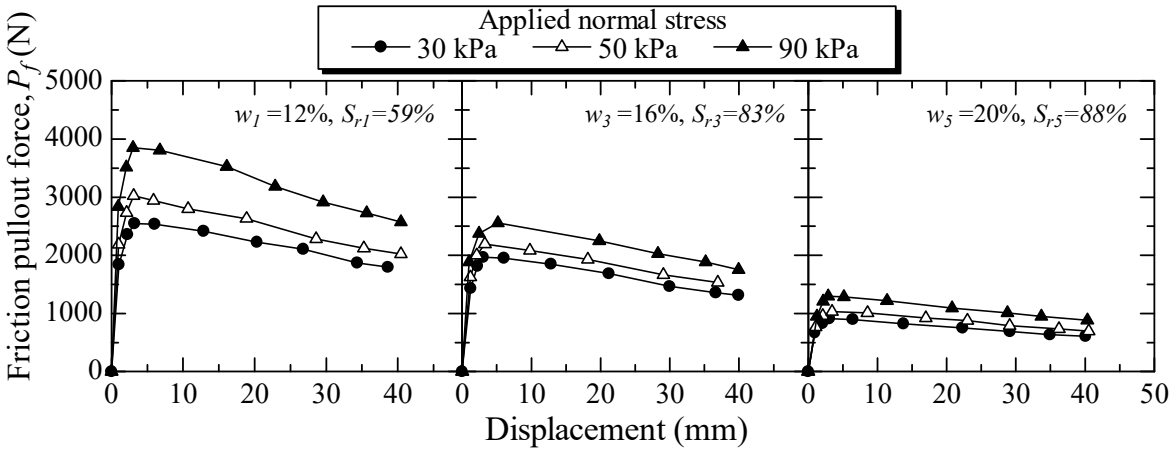

Figure 4 Pullout test results of a longitudinal member under different normal stresses.

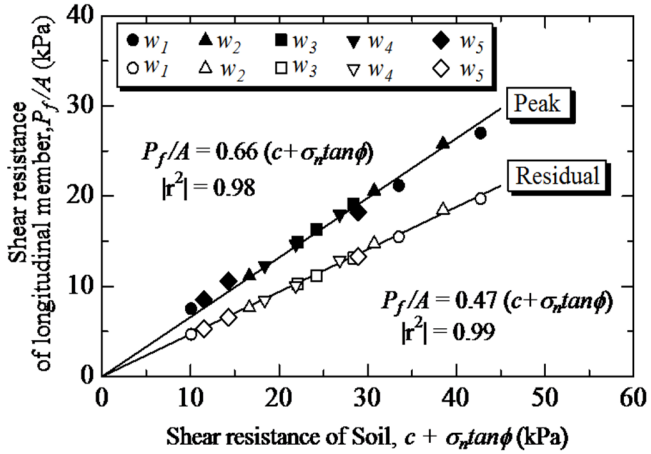

Figure 5 Relationship between shear interface and shear strength of red clay

4.3 Bearing Pullout Resistance

4.3.1 Bearing pullout resistance of a single isolated transverse member (n = 1)

The measured maximum bearing stress, σ_{bmax}, of a single transverse member for the red clay, with various dimensions (B and L) of transverse member and normal stresses is shown in Figure 6. By using the generalized equation (Eqs. (3)-(5)) to predict σ_{bmax}, the value of β can satisfactorily fit all the test data both on the dry and the wet sides of optimum of compacted red clay. This implied that the failure mechanism of the bearing reinforcement in red clay was punching shear for all water contents on both dry and wet sides of optimum. With the same punching shear failure mode and the significant reduction in shear strength with increasing water content, the bearing pullout resistance significantly decreased with increasing water content.

The analysis of the present and previous data (Sukmak et al., 2015 and 2016 and Horpibulsuk et al., 2016) leads to the 3 dimensional plot of β versus F and w/w_{OWC} as shown in Figure 7. The plot was made from the three assumptions.

1. At w = w_{OWC}, F = 45% is the threshold limit separating small and large change in bearing pullout resistance with F (Sukmak et al., 2015).
2. On the dry side of optimum and at w_{OWC}, the β is identical and can be determined from the following equation (Sukmak et al., 2015):

$$\beta_{(rad)} = \left[-0.00002F^2 + 0.0002F + 0.505\right]\pi \qquad \text{for } 20 < F < 98\% \qquad [11]$$

3. On the wet side of optimum, β reduces significantly with increasing w/w_{OWC} until $\beta = \pi/3$ (punching shear) at w/w_{OWC} = 1.33 (Sukmak et al., 2016; Horpibulsuk et al., 2017 and present data). Therefore the β at any w/w_{OWC} can be approximated using interpolation method where the β at w/w_{OWC} = 1 can be determined from Eq. (11).

With the known β value determined from Figure 7, the P_{b1} can be determined using Eqs.(3) to (5).

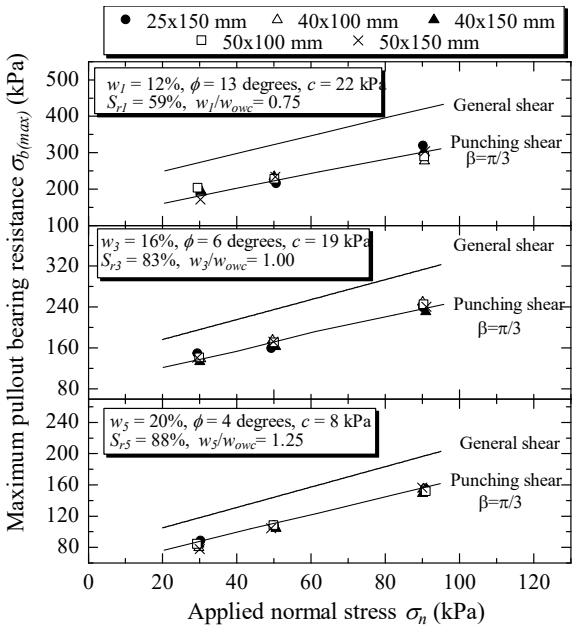

Figure 6 Maximum pullout bearing resistance of a single isolated transverse member at various water contents.

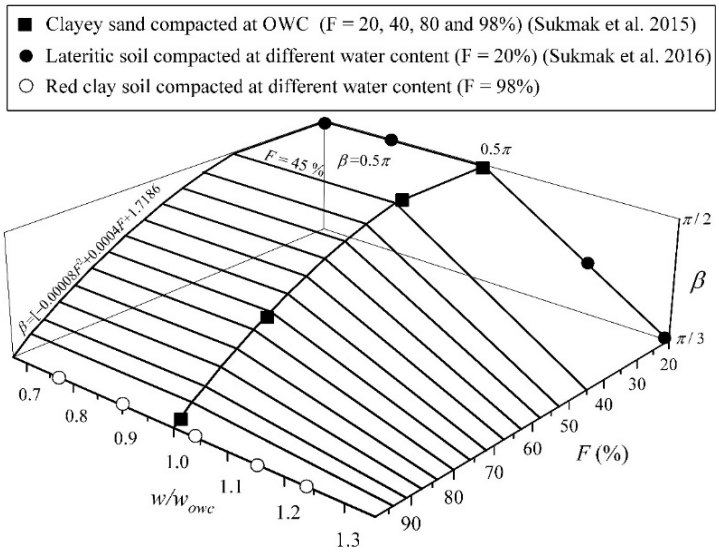

Figure 7 Plot of β versus F and w/w_{OWC}

4.4 RECOMMENDED METHOD FOR PREDICTING PULLOUT RESISTANCE

A stepwise procedure for assessing pullout bearing resistance with transverse members, n of 1 to 4 for various water contents and fines contents is proposed as follows:

Determine the friction pullout resistance of the bearing reinforcement

1. Perform sieve, compaction and direct shear tests on the backfill material to determine F, w_{OWC} and shear strength parameters.
2. Determine α for the friction pullout resistance, which can be directly obtained from a pullout test on a longitudinal member or approximated from Eq.(9) .
3. Determine the maximum pullout friction force of longitudinal member at required normal stress level from Eq. (1).

Determine the bearing pullout resistance of the bearing reinforcement

4. Determine β at required w and F using Figure 8.
5. Determine the N_c and N_q values using Eqs. (4) and (5).
6. Determine P_{b1} from $P_{b1} = N_q \sigma_n BL$.
7. Determine the maximum pullout bearing force with n transverse members (without interference between transverse members), P_{bn} from $P_{bn} = nP_{b1}$.

Determine the pullout resistance of the bearing reinforcement

10. Determine the pullout resistance = $P_f + P_{bn}$.

5. CONCLUSIONS

This research investigated the combined effects of fines and water contents on the pullout resistance of bearing reinforcement embedded in the cohesive-frictional soils. The previous and present test results were analyzed to develop the generalized pullout resistance predictive equations at various water contents and fines contents. The following conclusions can be drawn from this study:

1) The total pullout resistance of the bearing is the sum of friction pullout and bearing pullout resistances. The lower water content resulted in the higher shear strength; hence the higher pullout friction resistance. The peak and residual interaction factors (α_p and α_r) value were dependent upon F, irrespective of water contents. The relationships between α_p and α_r versus F were suggested in this paper. The relationships between α_p and α_r versus F are $\alpha_p = -0.002F + 0.859$ and $\alpha_r = -0.0014F + 0.592$, respectively.

2) The bearing pullout resistance of transverse members is calculated in terms of the number of transverse members (n) and pullout bearing resistance of a single transverse member . The Pb1 were found to be primarily controlled by F and w/w_{OWC}. The 3-dimensional plot of β versus w/w_{OWC} and F in the range of and 20 < F < 98% are proposed to determine Pb1. On the dry side of optimum and at w_{OWC}, the of is recommended for F < 45%. On the wet side of optimum, β reduces significantly with increasing w/w_{OWC} and F until $\beta = \pi/3$ at w/wOWC = 1.33.

3) The method of predicting pullout resistance of bearing reinforcement embedded in cohesive-frictional soils were proposed in this research. The proposed method is useful for examination of internal stability of BRE wall during construction and at the end of construction. The development of this generalized pullout resistance predictive equations for the bearing reinforcement is based on sound principle. The framework can be extended to develop pullout resistance predictive equations of other reinforcements for further study.

REFFERENCES

AASHTO, 2002. Standard Specifications for Highway Bridges, seventeenth ed. American Association of State Highway and Transportation Offcials, Washington, DC, USA.

ASTM D698-91, 1995. Test method for laboratory compaction characteristics of soil using starndard effort (12,400 ft-lbf/ft3 (600 kN-m/m3)). Annual book of ASTM standards 04.08, 69-76.

Bergado, D.T., Chai, J.C., Marui, H., 1996. Prediction of pullout resistance and pullout force displacement relationship for inectensible grid reinforcements. Soils and Founddations 36, 11-22.

Bonaparte, R., Christopher, B.R., 1987. Design and construction of reinforced embankments over weak foundations. Transportation Research Record 1153, 26–39.

Chai, J.C., 1992. Interaction between grid reinforcement and cohesive-frictional soil and performance of reinforced wall/embankment on soft ground. D.Eng. dissertation, Asian Institute of Technology, Bangkok, Thailand.

Chai, J.C., Miura, N., Shen, S.L., 2002. Performance of embankments with and without reinforcement on soft subsoil. Canadian Geotechnical Journal 39, 838-848.

Chinkulkijniwat, A., Horpibulsuk, S., Yubonchit, S., Rakkob, T., Goodary, R. and Arulrajah, A. 2015. Laboratory approach for faster determination of the loading-collapse yield curve of compacted soils. Journal of Materials in Civil Engineering, 04015148(1-8).

Fleming, I.R., Sharma, J.S., Jogi, M.B., 2006. Shear strength of geomembrane–soil interface under unsaturated conditions. Geotextiles and Geomembranes 24, 274-284.

Horpibulsuk, S., Niramitkronburee, A., 2010. Pullout resistance of bearing reinforcement embedded in sand. Soils and Founddations 50, 215-226.

Horpibulsuk, S., Suksiripattanapong, C., Niramitkornburee, A., Chinkulkijniwat, A., and Tangsutthinon, T. 2011. Performance of earth wall stabilized with bearing reinforcements. Geotextiles and Geomembranes 29, 514-524.

Horpibulsuk, S., Suksiripattanapong, C. and Chinkulkijniwat, A. 2013. Design method for bearing reinforcement earth wall. Geotechnical Engineering Journal 44(4), 125-131.

Horpibulsuk, S., Suddeepong, A., Chamket, P., Chinkulkijniwat, A., 2012. Compaction behavior of fine-grained soils, lateritic soils and crushed rocks. Soils and Foundations 53, 166-172.

Horpibulsuk, S., Suksiripattanapong, C., Niramitkronburee, A., Chinkulkijniwat, A., Tangsuttinon, T., 2011. Performance of earth wall stabilized with bearing reinforcements. Geotextiles and Geomembranes 29, 514-524.

Horpibulsuk, S., Udomchai, A., Joongklang, A., Chinkulkijniwat, A., Mavong, N., Suddeepong, A., Arulrajah, A., 2016. Pullout resistance mechanism of bearing reinforcement embedded in residual clayey soils. Geosynthetics International 24(3), 255-263.

Jewell, R.A., Milligan, G.W.E., Sarsby, R.W., Dubois, D., 1984. Interaction between soil and geogrids. Proceedings of the sympositum on Polymer Grid Reinforcement in Civil Engineering, Thomas Telford Limited, London, UK, 11-17.

Jewell, R.A., 1988. The mechanics of reinforced embankments on soft soils. Geotextiles and Geomembranes 7, 237–273.

Jiang, Y., Han, J., Parsons, R.L., Brennan, J.J., 2016. Field instrumentation and evaluation of modular-block MSE walls with secondary geogrid layers. J. Geotech. Geoenviron. Eng. http://dx.doi.org/10.1061/(ASCE)GT.1943-5606.0001573, 05016002.

Liu, C.N., Ho, Y.H., Huang, J.W., 2009. Large scale direct shear tests of soil/PET-yarn geogrid interfaces. Geotextiles and Geomembranes 27, 19-30.

Liu, H., 2012. Long-term lateral displacement of geosynthetic-reinforced soil segmental retaining walls. Geotextiles and Geomembranes 32, 18-27.

Mohamed, S.B.A., Yang, K.-H., Hung, W.-Y., 2013. Limit equilibrium analyses of geosynthetic-reinforced two-tiered walls: calibration from centrifuge tests. Geotextiles and Geomembranes 41.

Oloo, S.Y., Fredlund, D.G., 1996. A method for determination of ϕb for statically compacted soils. Canadian Geotechnical Journal 33, 272-280.

Palmeira, E.M., 2004. Bearing force mobilisation in pull-out tests in geogrids. Geosynth. Int 22, 481-509.

Perterson, E.M., Anderson, L.R., 1980. Pullout resistance of welded wire mats embedded in soil. Research Report Submitted to Hilfiker Co, from the Civil and Environmental Engineering Department, Utah State University, USA.

Potyondy, J.G., 1961. Skin friction between various soil and construction materials. Geotechnique 6, 339-353.

Roodi Gholam, H., Zornberg Jorge, G., 2017. Stiffness of Soil-Geosynthetic Composite under Small Displacements. II: Experimental Evaluation. Journal of Geotechnical and Geoenvironmental Engineering 143, 04017076.

Sukmak, P., Horpibulsuk, S. and Shen, S.L. 2013. Strength development in clay-fly ash geopolymer. Construction and Building Materials 40, 566-574.

Sukmak, K., Sukmak, P., Horpibulsuk, S., Chinkulkijiniwat, A., Arulrajah, A., Shen, S.L., 2016. Pullout resistance of bearing reinforcement embedded in marginal lateritic soil at molding water contents. Geotextiles and Geomembranes 44, 475-483.

Sukmak, K., Sukmak, P., Horpibulsuk, S., Han, J., Shen, S.L., Arulrajah, A., 2015. Effect of fine content on the pullout resistance mechanism of bearing reinforcement embedded in cohesiveefrictional soils. Geotextiles and Geomembranes 43, 107-117.

Suksiripattanapong, C., Chinkulkijniwat, A., Horpibulsuk, S., Rujikiatkamjorn, C., and Tangsuttinon, T. 2012. Numerical Analysis of Bearing Reinforcement Earth (BRE) Wall. Geotextiles and Geomembranes 32, 28-37.

Suksiripattanapong, C., Horpibulsuk, S., Chinkulkijniwat, A., Chai, J.C., 2013. Pullout resistance of bearing reinforcement embedded in coarse-grained soils. Geotextiles and Geomembranes 36, 44-54.

Udomchai, A., Horpibulsuk, S., Suksiripattanapong, C., Mavong, N., Rachan, R. and Arulrajah, A. 2017. Performance of the bearing reinforcement earth wall as a retaining structure in the Mae Moh mine. Geotextiles and Geomembranes, doi: 10.1016/j.geotexmem.2017.04.007.

Wang, S., Chan, D., Lam, K.C., 2009. Experinental study of the effect of fines content on dynamic compaction grouting depcomposed granic of Hong Kong. Construction and Building Materials 23, 1249-1264.

Zhang, N., Shen, S.L, Wu, H.N., Chai, J.C., and Yin, Z.Y. 2015. Evaluation of performance of embankments with reinforcement on PVD-improved marine clay, Geotextiles and Geomembranes, 43(6), 506-514.